The Astrophysical Journal, 642:427–437, 2006 May 1

CLOSE BINARY INTERACTIONS OF INTERMEDIATE-MASS BLACK HOLES: POSSIBLE ULTRALUMINOUS X-RAY SOURCES?

L. Blecha,[1] N. Ivanova,[1] V. Kalogera,[1] K. Belczynski,[2] J. Fregeau,[1] and F. Rasio[1]

Received 2005 August 27; accepted 2005 December 22

ABSTRACT

While many observed ultraluminous X-ray sources (ULXs; $L_X \geq 10^{39}$ ergs s^{-1}) could be extragalactic X-ray binaries (XRBs) emitting close to the Eddington limit, the highest luminosity ULXs ($L_X > 3 \times 10^{39}$ ergs s^{-1}) exceed the isotropic Eddington luminosity for even high-stellar-mass–accreting black hole XRBs. It has been suggested that these highest luminosity ULXs may contain accreting intermediate-mass black hole (IMBH) binaries. We consider this hypothesis for dense, young ($\sim$100 Myr) stellar clusters where we assume that a 50–500 $M_\odot$ central IMBH has formed through runaway growth of a massive star. We develop numerical simulations of such clusters' cores by combining single and binary star evolutionary syntheses with a simple treatment of dynamical interactions. We model interactions of the IMBH with single and binary stars, as well as single-binary and binary-binary interactions, but not the formation of a cusp around the IMBH. The core density and velocity dispersion are assumed to be constant over 100 Myr. We investigate the succession of IMBH binary companions and the evolution of their orbital parameters to obtain estimates of the incidence of mass transfer phases and possible ULX activity involving the IMBH. We find that although it is common for the central black hole to acquire binary companions, there is a very low probability that these interacting binaries will become observable ULX sources.

Subject headings: binaries: close — black hole physics — galaxies: star clusters — X-rays: binaries

1. INTRODUCTION

Extragalactic observations with the *Einstein Observatory* space X-ray telescope revealed a new category of sources, currently known as ultraluminous X-ray sources (ULXs; Fabbiano 1989). In 1990, surveys conducted with the *Röntgensatellit* (*ROSAT*) were able to resolve many of these sources as distinct objects not associated with emission from galactic nuclei. Up to half of the galaxies surveyed were found to contain off-nuclear ULXs (Colbert & Mushotzky 1999; Roberts & Warwick 2000; Lira et al. 2000; Colbert & Ptak 2002; Colbert & Miller 2006). In analogy with X-ray sources observed in our own Galaxy, many ULXs could be extragalactic X-ray binaries (XRBs) with stellar-mass black hole (BH) accretors (e.g., Rappaport et al. 2005). However, in many cases their luminosities exceed the Eddington limit for isotropic emission from an accreting stellar-mass BH. The lowest luminosity that commonly defines a ULX, $L_X \geq 10^{39}$ ergs s^{-1}, corresponds to an Eddington black hole mass $\gtrsim 8\ M_\odot$, still within the BH mass range allowed by stellar evolution models. Based on the X-ray survey conducted by Colbert & Ptak (2002), ULXs with $L_X \geq 10^{39}$ ergs s^{-1} are estimated to exist in $\sim$12% of all galaxies (Ptak & Colbert 2004). Of the 87 X-ray (2–10 keV) sources observed, 45 had $L_X > 3 \times 10^{39}$ ergs s^{-1}. This corresponds to the Eddington luminosity for the highest mass black holes that can form through single-star collapse, $\sim 25\ M_\odot$ for a metallicity of $Z = 0.001$ (Belczynski et al. 2004). We see that as much as half of this observed ULX population requires an alternative to the model of isotropic emission from a stellar-mass XRB.

Observations increasingly support the idea that some ULX sources may harbor intermediate-mass black holes (IMBHs; Colbert & Mushotzky 1999; for a critical review see Mushotzky 2004). Until recently, no evidence existed for BHs in the wide mass range between stellar-mass and supermassive BHs. Many spectral and timing observations conducted with the *Chandra X-Ray Observatory*, *Advanced Satellite for Cosmology and Astrophysics* (*ASCA*), and *XMM-Newton* have confirmed that ULXs are not associated with supernovae and are consistent with accreting binaries (Fabbiano & White 2006). In addition, ULX positions are strongly correlated with young, star-forming regions. Examples include the nine ULXs found in the Antennae (Fabbiano et al. 2001) and the highest luminosity ULX yet observed, in M82 (peak $L_X \sim 9 \times 10^{40}$ ergs s^{-1}, corresponding to an IMBH mass $\simeq$700 $M_\odot$ if $L_X \simeq L_X^{\rm Edd}$; Kaaret et al. 2001; Matsumoto et al. 2001). The young, dense clusters where ULXs are often observed are also likely sites for IMBH formation (Freitag et al. 2006a, 2006b; Gürkan et al. 2004).

Accretion disk spectra provide a further test for the presence of IMBHs: higher mass BHs are expected to have cooler accretion disks modeled as multicolor disks (Mitsuda et al. 1984). Some evidence for low-temperature disks was recently found using high-resolution *XMM-Newton* spectra of numerous ULXs, including those in NGC 1313, NGC 4559, Holmberg IX, and the Antennae (Miller et al. 2003, 2004a, 2004b). As Colbert & Miller (2006) note, the sources observed to have cool disks are also those with luminosities too high to be explained by XRBs, even if they are beamed XRBs. Nevertheless, we note that X-ray spectral interpretation is subject to a number of model assumptions and may not be unique.

Anisotropic, or beamed, disk emission is another possible explanation for apparently super-Eddington X-ray luminosities. The degree to which emission is beamed can be defined by the beaming fraction $b = \Omega/4\pi$, where Ω is the solid angle of emission. ULXs containing beamed stellar-mass XRBs could be a short phase of rapid mass transfer in the lifetime of ordinary XRBs, such as thermal-timescale mass transfer (King et al. 2001). As demonstrated by King et al. (2001), by introducing mild beaming, the

[1] Northwestern University, Department of Physics and Astronomy, 2131 Tech Drive, Evanston, IL 60208; l-blecha@alumni.northwestern.edu, nata@northwestern.edu, vicky@northwestern.edu, fregeau@northwestern.edu, rasio@northwestern.edu.

[2] Tombaugh Fellow, Department of Astronomy, New Mexico State University, Las Cruces, NM 88003; kbelczyn@nmsu.edu.

XRB falls within the stellar-mass BH range, assuming $L_X < 10^{40}$ ergs s^{-1}. However, about 5%–10% of the total ULX population is observed to have $L_X \geq 10^{40}$ ergs s^{-1} (Colbert & Miller 2006; Ptak & Colbert 2004; Colbert & Ptak 2002). At these luminosities, very massive BHs ($\sim$25 $M_\odot$) could fall below the Eddington limit with $b \lesssim 0.25$. To have the required mass ratio $q = M_2/M_1 > 1$, where M_1 is the BH mass, these BHs would require a very massive companion. More moderate mass BHs would require more severe beaming fractions that are not easily justified. Furthermore, in at least two instances observations seem to indicate isotropic X-ray emission. These include an isotropic nebula observed around the ULX in Holmberg II (Pakull & Mirioni 2001) and the discovery of quasi-periodic oscillations (QPOs) from the brightest ULX in M82 (Strohmayer & Mushotzky 2003).

Transient behavior of a ULX source is an important test for the presence of an IMBH (Kalogera et al. 2004). If the ULX is a beamed stellar-mass XRB in thermal-timescale mass transfer, it is expected to produce persistent emission at or above the Eddington luminosity (King et al. 2001). A persistent IMBH ULX similarly would require a sustained $\dot{M}$ comparable to the Eddington mass transfer rate,

$$\dot{M}_{\rm Edd} \simeq 2.3 \times 10^{-9} \left(\frac{M_{\rm IMBH}}{M_\odot} \right) M_\odot \ {\rm yr}^{-1}. \quad (1)$$

For the IMBH masses we consider, this is in excess of 10^{-7} $M_\odot$ yr^{-1}, corresponding to L_X of about a few $\times 10^{40}$ ergs s^{-1}. Transient IMBH ULX sources are more plausible because they confine the most extreme rates of mass transfer to short outburst periods. Admittedly, our current physical understanding of transient behavior is not complete. Nevertheless, it is generally accepted that an accreting binary becomes a transient when the mass transfer rate driven by the donor is lower than a certain critical value and a thermal disk instability develops. In what follows we adopt the critical mass transfer rate for transient behavior of an X-ray–irradiated disk given by Dubus et al. (1999),

$$\dot{M}^{\rm irr}_{\rm crit} \simeq 1.4 \times 10^{-9} \left(\frac{M_{\rm IMBH}}{M_\odot} \right)^{-0.4} \left(\frac{R}{R_\odot} \right)^{2.1} \times \left(\frac{C}{5 \times 10^{-4}} \right)^{-0.5} M_\odot \ {\rm yr}^{-1} \quad (2)$$

for a disk of radius R, where C is assumed to be 5×10^{-4} for most donors. It can also be shown that the critical $\dot{M}$ for transience corresponds to a minimum black hole mass that depends on companion mass and orbital period (King et al. 1996). As Kalogera et al. (2004) have shown, this minimum BH mass is high for main-sequence (MS) donor stars (10^3 $M_\odot$ on average for a 10 $M_\odot$ donor). Red giant (RG) donors can more easily form transient systems with IMBHs. One should note that due to the minimum mass limit, a stellar-mass BH binary is unlikely to be transient, so any transient ULX observed is a strong IMBH candidate.

In our simulations, we consider IMBHs that have formed through "runaway collisions" of MS stars. This is a channel for IMBH formation in which a series of rapid mergers occur as the cluster begins core collapse, causing growth of a central massive object that can collapse to a black hole (Portegies Zwart et al. 1999; Portegies Zwart & McMillan 2002; Gürkan et al. 2004; Freitag et al. 2006a, 2006b). It has been suggested that an IMBH formed through runaway growth actually prevents core collapse and causes the core to reexpand (Baumgardt et al. 2004). In the dense clusters we are considering, the timescale for IMBH formation through runaway mergers is estimated to be $\lesssim$3 Myr (Portegies Zwart & McMillan 2002; Gürkan et al. 2004). Because the core collapse time, $t_{\rm cc}$, is expected to obey the relation $t_{\rm cc} \sim 0.15 t_{\rm rc}(0)$, where $t_{\rm rc}(0)$ is the initial core relaxation time, this constrains $t_{\rm rc}$ to be $\lesssim$30 Myr (Gürkan et al. 2004).

Given that a plausible IMBH formation method exists, the question most pertinent to understanding ULXs is whether an IMBH, once formed, will gain close stellar companions that can sustain mass transfer at ULX X-ray luminosities. No prior studies have attempted to investigate numerically with both dynamics and binary evolution whether binary formation and mass transfer can occur with IMBHs in a dense cluster core (for an analytical exploration of tidal capture and its consequences, see Hopman et al. 2004). Here we take the first step in studying IMBH binary interactions as a ULX possibility, using detailed numerical simulations that combine dynamical interactions with full binary stellar evolution. In § 2 we outline the details of our simulations. The results for our standard cluster model (details below) are presented in § 3. The variations of these results for other cluster models are described in § 4. In § 5, we discuss our results, estimating a lower limit on the incidence of IMBH mass transfer, and we outline our goals for future simulations.

2. CLUSTER SIMULATIONS WITH CENTRAL IMBH

The goal of our simulations is to examine the ability of IMBHs in young, dense stellar clusters to form and maintain close binary systems with companion stars. We employ a numerical code developed by Ivanova et al. (2005, where a detailed description of the method can be found). This adopted hybrid code incorporates (1) a stellar population synthesis code to evolve single stars and binary systems (StarTrack; Belczynski et al. 2002, 2006); (2) a semianalytical prescription for two-, three-, and four-body stellar collisions, disruptions, exchanges, and tidal captures based on previously derived cross sections; and (3) a numerical toolkit for direct N-body integration of three- and four-body systems (FEWBODY; Fregeau et al. 2004).

This combination provides us with a unique numerical tool that lends itself to the study of binary interactions in cluster cores. At the young cluster ages that we consider, large-scale cluster evolution has little effect, so certain simplifications can be made. The cluster density profile is assigned by dividing the cluster into two regions: a dense core and an outer halo. In the context of this model, which is qualitatively based on mass segregation, we employ a "fixed background" in which the core's stellar number density n_c and velocity dispersion σ remain constant over the simulation time (see also, e.g., Hut et al. 1992; Di Stefano & Rappaport 1994; Sigurdsson & Phinney 1995; Portegies Zwart et al. 1997a, 1997b; Rasio et al. 2000). These simplifying assumptions are necessary at present in order to incorporate both binary evolution, with all its complications, and basic dynamics in these young, IMBH-containing clusters. However, recent results of purely dynamical simulations of clusters with an IMBH presented by Trenti et al. (2006) clearly support the assumption of constant core properties over the simulation time (100 Myr; see their Fig. 1). They also find that the binding energies of binaries in the core do not correlate with position (see their Fig. 2), lending tentative support to the assumption of uniform core properties. Last, we note that we do not follow the long-term evolution of multiple systems other than binaries, and therefore we cannot follow the formation and evolution of a cusp around the IMBH.[3]

[3] Such a cusp is expected to form over a time of the order of the core relaxation time ($t_{\rm rc}$; Merritt & Szell 2006). In our simulations, which last for $\sim 3 t_{\rm rc}$, we therefore consider the very early times during and after cusp formation.

In our models, an IMBH is added to the core at 1 Myr, in accordance with estimated IMBH formation times of 1–3 Myr in clusters (Portegies Zwart & McMillan 2002). To form an IMBH through runaway collisions, the initial core relaxation time, $t_{\rm rc}$, must be $\lesssim$25–30 Myr (Gürkan et al. 2004). This time is given by (Spitzer 1987)

$$t_{\rm rc} = \frac{\sigma_{\rm 3D}^3}{4.88\pi G^2 \ln(\gamma N) n_c \langle m \rangle^2}, \quad (3)$$

where $\sigma_{\rm 3D}$ is the three-dimensional velocity dispersion, n_c is the core number density, N is the total number of stars, $\langle m \rangle$ is the average stellar mass, and γ, the coefficient in the Coulomb logarithm $\Lambda = \gamma N$, is assumed to be 0.01 (e.g., Gürkan et al. 2004). For our standard model (parameters are described below), $t_{\rm rc} \simeq$ 29 Myr, in good agreement with the constraint for runaway collisions.

We evolve the clusters to 100 Myr, as we consider only young clusters like those with which ULXs are most often associated. We can then neglect long-term contributions of the outer halo to cluster evolution and synthesize the entire stellar population of $N = 2.7 \times 10^4$ in the core. Mass segregation within the core is incorporated through our choice of the initial mass function (IMF) used for the stellar population in the core.

An initial binary fraction of 100% is assumed, which provides the maximum possible concentration of binaries to interact with and become companions of the IMBH. Observations indicate that young clusters are expected to have very high binary fractions (Levine et al. 1999; Apai 2004; Delgado-Donate et al. 2004). This assumption is also consistent with the suggestion that cluster binary populations are depleted over time by interactions and stellar evolution (Mikkola 1983; Hills 1984; Bacon et al. 1996; Fregeau et al. 2004; Ivanova et al. 2005). Initial conditions for binary orbital parameters are assigned as outlined in § 3.1 of Ivanova et al. (2005), with slight modifications:

1. The binary mass ratio $q = M_2/M_1$ is assigned a uniform distribution $0 < q < 1$, where M_1 and M_2 are the binary primary and secondary, respectively.
2. A uniform logarithmic distribution is used for the binary period, P, ranging from 0.1 to 10^7 days.
3. The thermal distribution is used for the binary eccentricities e with probability density $\rho(e) = 2e$.
4. Binary systems are rejected from the initial distribution if one of the binary components enters Roche lobe overflow (RLOF) at pericenter.
5. We use the IMF of Kroupa (2002) for primary stars between 0.8 and 100 $M_\odot$ in most simulations.
6. Secondary stars are restricted in a mass range between 0.05 and 100 $M_\odot$.

Our standard cluster model (model A; see Table 1) has a one-dimensional stellar velocity dispersion $\sigma = 10$ km s^{-1} and a core stellar number density $n_c = 1.33 \times 10^5$ pc^{-3}. The latter corresponds to a luminosity density $\geq 10^7\ L_\odot$ pc^{-3} for a cluster age $\leq 10^8$ yr. The total cluster mass is $\simeq 5 \times 10^4\ M_\odot$. We use 100 $M_\odot$ as our standard IMBH mass, but we explore a range of IMBH masses from 50 to 500 $M_\odot$ (see § 4.1). Note that each type of simulation must be repeated many times to obtain good statistics.

We also consider two variations of our standard cluster model (see Table 1): with model B we explore the effect of a flatter IMF, and with model C we examine results for less dense clusters. Detailed simulations of clusters that form an IMBH just before core collapse have shown that rapid mass segregation preceding IMBH formation creates a mass function flatter than Kroupa's for stars >5–10 $M_\odot$ (Gürkan et al. 2004; Freitag et al. 2006a; M. Freitag 2005, private communication). These results have prompted us to consider the effects of mass segregation on the formation of IMBH binaries. We have also examined whether any Brownian-like motion of the IMBH would cause it to interact with stellar populations that have properties different than those typical of the compact cluster cores. Assuming energy equipartition exists between the IMBH and the cluster, the IMBH in a constant-density core will experience radial oscillations of amplitude (Bahcall & Wolf 1976)

TABLE 1
Cluster Models

Model	IMF	n_c (pc^{-3})
A	Kroupa	1.33×10^5
B	Flattened	1.33×10^5
C	Kroupa	1.33×10^4

Notes.—The IMF in model B is a broken power-law mass function $\xi(M) \sim M^\alpha$, with $\alpha = -1.25$ for $0.8 < M/M_\odot < 5$ and $\alpha = -1.5$ for $M/M_\odot > 5$. Models A and B were tested with and without 3BBF. Model A is also tested with a range of IMBH masses from 50 to 500 $M_\odot$.

$$R \simeq \frac{R_{\rm core}}{\sqrt{3}} \left(\frac{M_{\rm IMBH}}{M_{\rm tot}} \right)^{1/2}, \quad (4)$$

where $R_{\rm core}$ is the core radius, $M_{\rm IMBH}$ is the IMBH mass, and $M_{\rm tot}$ is the total mass of the rest of the cluster. For a 100 $M_\odot$ IMBH and total cluster mass $\simeq 5 \times 10^4\ M_\odot$, we obtain an oscillation amplitude that is safely small: $R/R_{\rm core} \simeq 2.5\%$.

We do not normally allow binary formation through three-body interactions in any of our simulations, as the initial binary fraction is 100%, but we do test the effect of three-body binary formation (3BBF) on models A and B. The details of our treatment of 3BBF are given in Ivanova et al. (2005).

A large fraction of IMBH binaries acquire at least one and often a series of tertiary objects; however, no population synthesis code currently exists that is capable of modeling full stellar evolution for triple systems. For triple systems that are considered stable after the detailed direct N-body modeling with FEWBODY (see stability criterion in Mardling & Aarseth 2001), we implement a "breakage" prescription that is physically self-consistent. The energy required to eject the outer star is obtained by shrinking the inner binary orbit. The outer star is released unless the inner binary merges during shrinkage; in this case the inner system is allowed to merge and the outer companion is kept at its new, wider orbit to form the final binary system. The condition for merger is that the stars in the inner binary are in physical contact at pericenter, or in the case of an IMBH binary, the secondary star enters the black hole's tidal radius

$$R_{\rm tidal} \approx R_{\rm comp} \left(\frac{M_{\rm IMBH}}{M_{\rm comp}} \right)^{1/3}. \quad (5)$$

We recognize that this artificial treatment can affect the evolution of IMBH binaries, for example, by preventing eccentricity boosts via the Kozai mechanism (Kozai 1962). For this reason we have undertaken a careful analysis of triple breaking and its effect on our results (see § 3.5). It should also be noted that in some cases with a RG companion, release of the outer

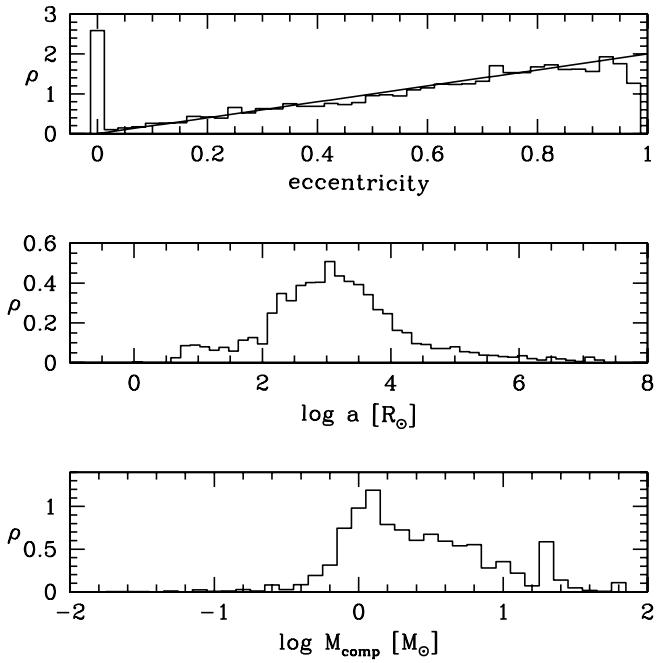

FIG. 1.—Probability densities of IMBH binary properties throughout the simulations: companion mass, orbital separation, and eccentricity. The thermal distribution, $\rho(e) = 2e$, is shown on the eccentricity plot. Results from 167 simulations of model A with a 100 $M_\odot$ IMBH are shown.

TABLE 2
IMBH BINARY COMPANIONS

Parameter	Value
MC runs[a]	167
$\langle N_{\rm comp}\rangle$[b]	6.49
$\langle N_{\rm MS}\rangle$[c]	5.90
$\langle N_{\rm post\text{-}MS}\rangle$[c]	0.47
$\langle N_{\rm MS}^{\rm MT}\rangle$[d]	0.26
$\langle N_{\rm post\text{-}MS}^{\rm MT}\rangle$[d]	0.23
MS MT companions[e]	4.36%
Post-MS MT companions[e]	50.00%
$t_{\rm comp}$[f]	57.63%
$t_{\rm MS}$[g]	40.87%
$t_{\rm post\text{-}MS}$[g]	4.44%
$t_{\rm MS}^{\rm MT}$[h]	2.81%
$t_{\rm post\text{-}MS}^{\rm MT}$[h]	0.11%

NOTE.—All simulations adopt cluster model A and $M_{\rm IMBH} = 100\ M_\odot$.
[a] Number of distinct Monte Carlo simulations evolved to 10^8 yr.
[b] Average number of companions (of any type) per run.
[c] Average number of companions of each type per run. Most post-MS companions are captured while on the MS and do not correspond to different stellar companions.
[d] Average number of MS and post-MS companions that undergo mass transfer per run.
[e] Percent of MS and post-MS companions that undergo mass transfer.
[f] Average percent of total simulation time spent with a companion of any type.
[g] Average percent of time with MS and post-MS companions.
[h] Average percent of time spent in MS and post-MS mass transfer phases.

companion induces a common-envelope phase in the resulting binary.

3. RESULTS FOR STANDARD MODEL

In what follows we present the results of our standard, 100 $M_\odot$ IMBH cluster simulations (model A in Table 1) in the context of the formation of IMBH binaries that experience mass transfer and may become observable as ULXs. In § 3.1 we discuss the characteristics of IMBH companions, including their orbital parameters, evolutionary types, and mass transfer phases. In § 3.2 we present an example of a single simulation and more details on the history of the IMBH. In § 3.3 we examine the X-ray luminosities produced by mass transfer and determine the time fraction over which the IMBH could be observable as a ULX. In § 3.4 we comment on the statistical interpretation of our results. Finally, in § 3.5 we analyze triple stellar systems and their possible effect on mass-transferring binaries.

3.1. *Statistical Results on IMBH Companions*

The distributions of three orbital parameters, companion mass, orbital separation, and eccentricity, are shown in Figure 1 for all 100 $M_\odot$ IMBH simulations for cluster model A. The prevalence of low-mass companions ($\sim$1 $M_\odot$) in the core is consistent with the model IMF that is dominated by such low-mass stars. Orbital separations of the dynamically formed IMBH binaries range widely from $\sim$1 to 10^7 $R_\odot$. The lower limit corresponds to the Roche lobe radius of the IMBH companion. On the other end, the soft boundary for binaries is defined as the "escape radius,"

$$a_{\rm soft} = \frac{GM_{\rm IMBH}}{\sigma^2} \simeq 10^5\ R_\odot. \quad (6)$$

In the simulations, a star is treated as a companion if its orbital separation is less than $100a_{\rm soft}$, corresponding to the maximum orbital separation, 10^7 $R_\odot$. Figure 1 illustrates that the majority of IMBH companions have orbital separations between 100 and 10^4 $R_\odot$. Eccentricities follow the initial thermal distribution, which favors higher values (Fig. 1). These high eccentricities tend to increase the occurrence of mass transfer events in which the companion overflows its Roche lobe at pericenter.

We find that the IMBH has a companion for $\simeq$60% of the total simulation time and that it has a mass-transferring companion for only $\simeq$3% of the total evolution time (Table 2). Figure 2 shows companion masses and orbital characteristics for different evolutionary types. The IMBH companions are overwhelmingly MS stars due to the much longer lifetime of this phase and their dominance by number. About 90% of unique 100 $M_\odot$ companions are MS stars for at least part of their binary lifetime; the IMBH has an average of $\sim$6 MS companions per simulation and only one post-MS companion for every two simulations. ("Post-MS" henceforth refers to all post–main-sequence evolutionary types capable of driving mass transfer; i.e., neutron stars [NSs] and BHs are excluded.) In contrast, post-MS companions are more likely candidates for RLOF than are MS companions. The percentage of post-MS companions that undergo mass transfer in our simulations is much higher than the percentage of mass-transferring MS companions (see Table 2). As noted above, post-MS companions are also more likely to enter transient mass transfer phases, which are more conducive to ULX formation. However, because the MS lifetime is about 10 times longer, mass transfer phases of MS companions are typically of longer duration, and the *numbers* of MS and post-MS mass-transferring companions per simulation are comparable (Table 2).

3.2. *Single Run Example*

The binary companion history of a single 100 $M_\odot$ IMBH simulation, using model A, is shown in Figures 3 and 4. This simulation is atypical in that it has multiple mass transfer events, but the behavior of these events is characteristic of mass transfer

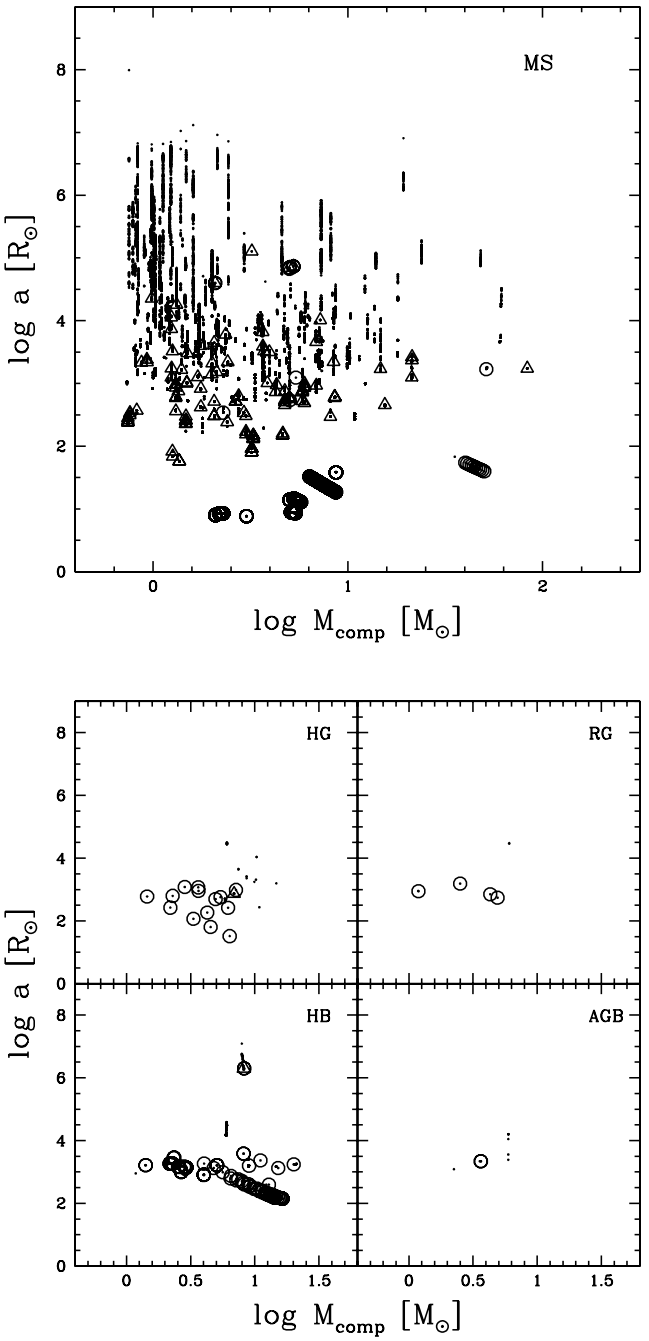

FIG. 2.—Companion mass vs. orbital separation for 42 model A simulations with a 100 $M_\odot$ IMBH, presented separately for the following companion evolutionary types: MS, Hertzsprung gap (HG), first giant branch (RG), horizontal branch (HB), and asymptotic giant branch (AGB). Fewer He and WD companions undergo mass transfer, and they are not included here. Dots denote simulation time steps when the IMBH has a binary companion. Open circles denote a mass-transferring companion (through RLOF). Open triangles denote binary companions associated with a triple system that was broken.

seen in other simulations. Figure 3 shows the IMBH evolution over time. The black hole has a companion for ~60% of its total evolution time, which is about the average that we calculate for all 100 $M_\odot$ simulations (Table 2). Note the often high eccentricities of non–mass-transferring companions, which is also typical of our simulations (Fig. 1). In the bottom panel of Figure 3, one can see the hardening of several companion orbits before they are disrupted by another interaction. The long mass transfer phase at the end of the simulation characterizes stable, MS mass transfer.

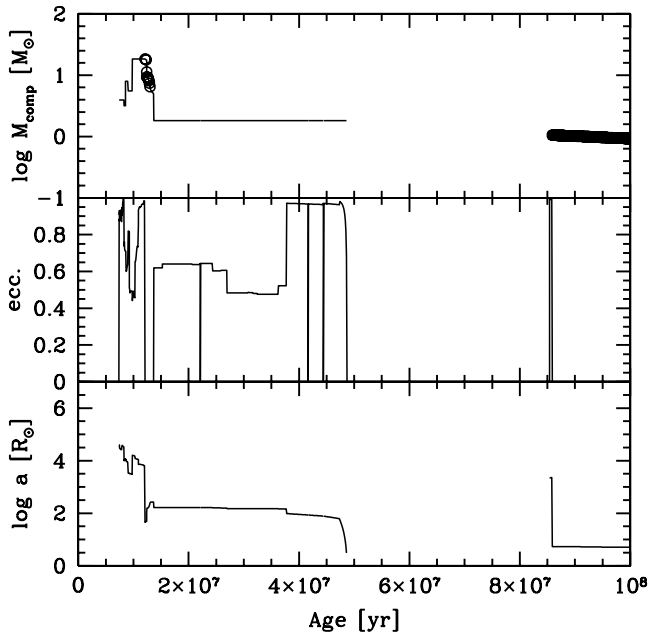

FIG. 3.—Evolutionary history of a single 100 $M_\odot$ IMBH simulation. *Top*, IMBH companion mass M_2; *middle*, eccentricity; *bottom*, orbital separation. Circles denote time steps with mass transfer; each non–mass-transferring companion appears at a different mass value. It is evident that the IMBH changes multiple binary companions during a single cluster simulation. Gaps in the top and bottom plots indicate times with no IMBH companion.

The first companion that undergoes RLOF (at about 10^7 yr) is the most interesting. Mass transfer begins on the MS and continues through the Hertzsprung gap (HG) until the donor becomes a He HG star. After this, the star explodes and leaves a NS orbiting the IMBH (see also discussion by Patruno et al. 2005). The

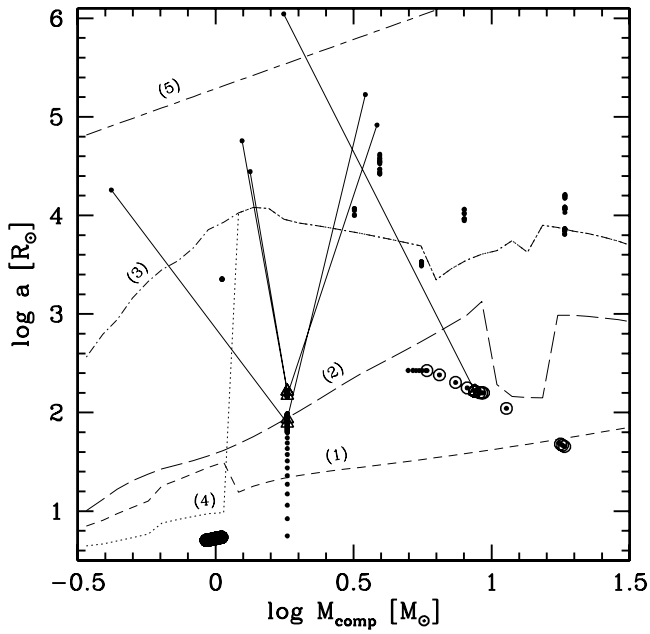

FIG. 4.—IMBH companion mass (M_2) vs. orbital separation (a) for the same simulation as shown in Fig. 1. Dots denote time steps with an IMBH companion; open circles denote mass-transferring companions. Triangles mark inner-binary orbital parameters of triple systems, and solid lines connect to the outer orbital parameters. The maximum companion orbit radii for RLOF are shown at the end of MS (*line 1*), the start of the RG branch (*line 2*), the maximum possible stellar radius (*line 3*), and the maximum stellar radius for clusters younger than 10^8 yr (*line 4*). Line 5 marks the soft/hard binary boundary.

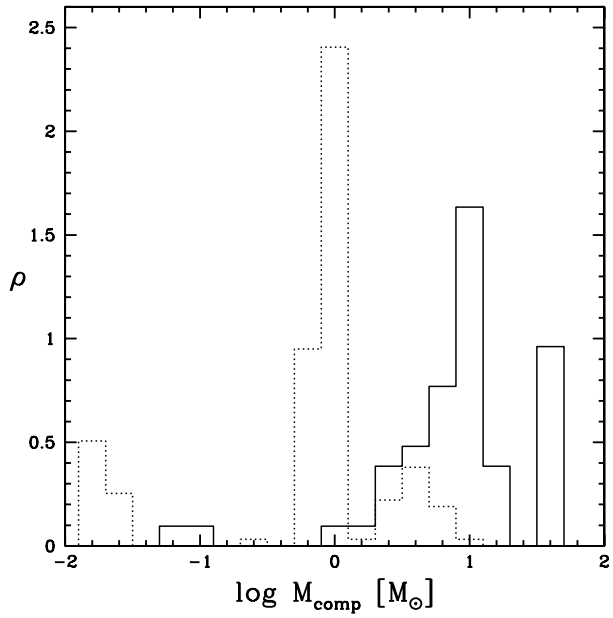

FIG. 5.—Distribution of companion masses during IMBH ULX phases for 80 standard model simulations with a 100 $M_\odot$ IMBH. The dotted line indicates companions in transient mass transfer, and the solid line indicates persistent mass transfer with $L_X \geq 10^{39}$ ergs s^{-1}.

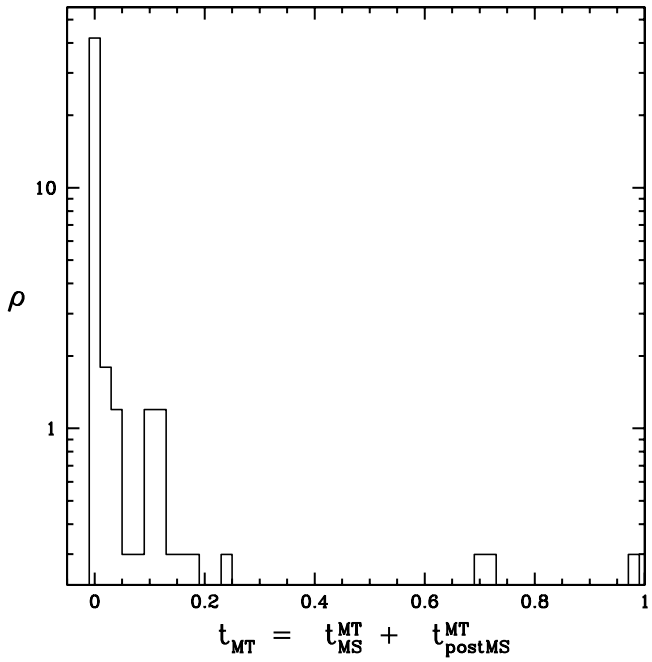

FIG. 6.—Distribution of mass transfer time fraction for 167 standard model simulations with a 100 $M_\odot$ IMBH.

companion's circularized orbit is kicked by the supernova to an eccentricity of about 0.6. As Figure 3 shows, the NS is later forced into an even higher e orbit by an encounter with an outer companion shown in Figure 4. This causes an eventual merger with the IMBH. The outer-companion swapping that occurs with the NS-IMBH binary is frequently observed behavior for a close, stable binary; more details on the behavior of triple systems are presented in § 3.5.

3.3. *X-Ray Luminosities*

We examine the range of X-ray luminosities produced by the various mass transfer phases that occur in our standard model simulations. The binary evolution component of the simulations allows us to calculate the mass transfer rate $\dot{M}$ driven by RLOF donors to the IMBH. We compare this rate to the critical rate $\dot{M}_{\rm crit}$ for transient behavior (eq. [2]) to determine whether the IMBH XRB is persistent or transient. If persistent, the transfer rate from the donor is converted to an expected X-ray luminosity; if transient, we assume that the XRB emits at its Eddington luminosity during disk outbursts (Kalogera et al. 2004; Ivanova & Kalogera 2006). In model A clusters with a 100 $M_\odot$ IMBH, the total mass transfer time fraction is about 3%. Of this, about 10% is spent under transient conditions, i.e., $\dot{M} < \dot{M}_{\rm crit}$. However, only a very small fraction of the transient mass transfer time, comparable to the transient duty cycle, will be spent in outburst. Observations of Galactic transients imply that this duty cycle is of the order of a few percent (McClintock & Remillard 2006). Such short duty cycles correspond to very low time fractions of the 10^8 yr cluster age that could be associated with ULX emission: <0.03%. The probability of detecting one of these transient sources in outburst is unfortunately vanishingly low. The other 90% of the mass transfer time in our simulations is persistent, and a ULX will result, by definition, if the X-ray luminosity exceeds 10^{39} ergs s^{-1}. We find that a 100 $M_\odot$ IMBH becomes a persistent ULX for only ~2% of total mass transfer time in model A clusters; this corresponds to ≃0.06% of the total age of the young clusters we consider here. We conclude that either persistent or transient IMBH ULXs would be observable for only a tiny fraction (<0.1%) of the cluster lifetime.

The mass distribution of IMBH companions as they evolve throughout the simulation time is shown in Figure 5, for all standard model simulations and for both transient and persistent ULX phases. Note that the persistent sources are in general fueled by more massive companions.[4] This is of particular relevance to recent observations of NGC 1313 X-2 that indicate the presence of two massive stars (10 and 20 $M_\odot$) in this highly luminous ($L_X \simeq 10^{40}$ ergs s^{-1}) ULX source (Mucciarelli et al. 2005). It is evident that such high-mass donors are not uncommon, even though the overall time fraction spent at ULX luminosities is very small.

3.4. *Averages versus Medians*

It should be emphasized that the mass transfer time fractions we present are averaged over all simulations and that individual simulations are given equal weight, but their results do vary over a wide range. The majority of our simulations have *no* IMBH mass transfer events at all; it turns out that the *median* mass transfer time fraction for each cluster model is always at or very near zero (Fig. 6). At the other extreme, IMBHs in a few model A simulations acquire very stable mass-transferring companions and spend more than half of their total evolution time in mass transfer phases. It is clear that the averages reported are affected by the presence of these rare outliers, as one can see by comparing the entire model A data set (Table 2, $t_{\rm MS}^{\rm MT}$ and $t_{\rm post\text{-}MS}^{\rm MT}$) to the smaller set for which triple system data were obtained, which does not include the outliers (Table 3, $t_{\rm MT}$). We would like to note that for the majority of our simulations the predictions for the IMBH binaries leading to mass transfer with X-ray luminosities in the ULX regime could be even lower than we report based on the average quantities and results. Ultimately, we chose to use time

[4] The very low mass companions at ~0.1 and ~0.01 $M_\odot$ are actually the same WD companion through a mass transfer phase that starts as persistent and ends in a transient stage; the WD has been brought into Roche lobe overflow by a dynamical interaction that pumped up the orbital eccentricity to ≃0.9.

TABLE 3
TRIPLE SYSTEMS AND IMBH COMPANIONS

Parameter	Value
MC runs[a]	109
$\langle N_{\rm trip}\rangle$[b]	3.46
$\langle N_{\rm trip}/N_{\rm bin}\rangle$[c]	0.50
Close triples[d]	28.90%
Affected MT companions[e]	47.72%
Close MT companions[f]	10.24%
$t_{\rm MT}$[g]	1.60%
$t_{\rm aff}^{\rm MTh}$	21.07%
$t_{\rm close}^{\rm MT\ i}$	4.96%

NOTE.—All simulations adopt cluster model A and $M_{\rm IMBH} = 100\ M_\odot$.
[a] Number of distinct Monte Carlo simulations for which triples data were obtained (note that Tables 3 and 5 are based on smaller sample sizes than are other data).
[b] Average number of unique triple systems per run.
[c] Average ratio of distinct triple systems to distinct binary systems formed.
[d] Percent of triples that are "close" ($p_{\rm out}/a_{\rm in} \leq 3$).
[e] Percent of mass transfer companions that are potentially affected by one or more tertiary companions gained during their lifetime.
[f] Percent of mass transfer companions that are potentially affected by one or more close tertiary companions gained during their lifetime.
[g] Percent of total simulation time spent in mass transfer phases.
[h] Percent of total mass transfer time potentially affected by triples.
[i] Percent of total mass transfer time potentially affected by close triples.

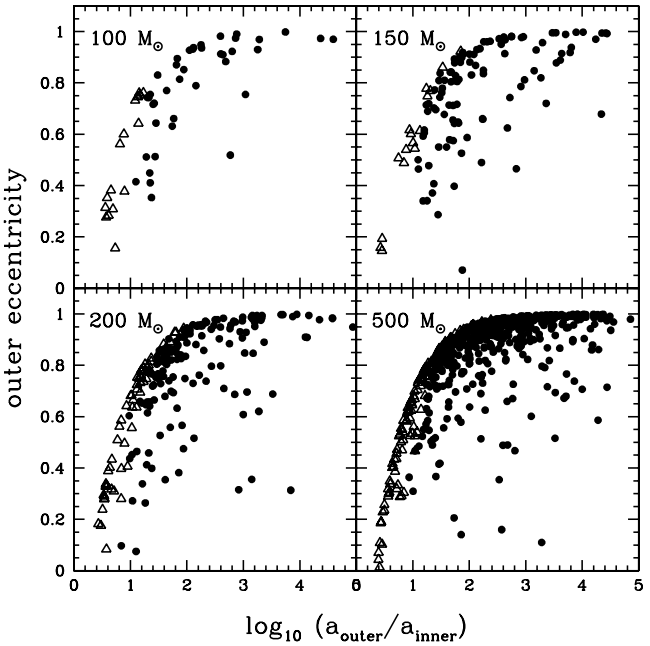

FIG. 7.—Triple systems formed for 16 simulations of 100, 150, 200, and 500 $M_\odot$ IMBHs. The outer orbit's eccentricity is plotted vs. the ratio of orbital separations for each triple system. Systems for which $p_{\rm out}/a_{\rm in} \leq 3$ are denoted by open triangles; other triples are shown by filled circles.

averages because they allow us to explore qualitative trends in the results (e.g., amount of MS vs. post-MS mass transfer). Since medians end up equal to zero, they are not useful for such explorations. Time averages also allow comparisons with observations in terms of ULX number occurrence in a large number of young clusters studied.

3.5. *Triple Systems*

The significant number of triple systems that form and are artificially (although physically self-consistently, i.e., conserving energy) disrupted in our simulations warrant a separate analysis of their possible effect on mass transfer. The NS merger event shown in the example simulation (Figs. 3 and 4), which resulted from an eccentricity boost by a third object, indicates that three-body interactions can play an important role even when triples are artificially broken. By analyzing the initial orbital characteristics of triples and their coincidence with mass transfer phases, we develop a sense of whether our treatment of triples is, in fact, a reasonable approximation.

Almost all of the triples are hard in the outer orbit (see Fig. 4), but depending on orbital parameters, the inner binaries may not be influenced by the outer companion. We quantify the degree of possible companion interaction using the ratio of the outer orbit's pericenter to the inner orbit's apocenter ($p_{\rm out}/a_{\rm in}$), that is, the closest possible approach between the two bodies. The result is shown in Figure 7 (*top left*) and in Table 3. We assign $p_{\rm out}/a_{\rm in} \leq 3$ as the critical value of this ratio, below which it is likely that the outer companion will have a nonnegligible effect on the inner binary. These "close" systems comprise less than $\frac{1}{3}$ of all triples.

Another diagnostic for triple systems is to calculate the percentage of mass transfer phases potentially affected. We consider mass transfer that follows or coincides with triple formation to be "affected" mass transfer. More importantly, we also calculate the percentage of mass transfer phases associated with close triples. While almost half of mass-transferring companions are affected, only ~10% are affected by close triples (Table 3). If we instead consider the total mass transfer *time* that is similarly affected, this fraction drops to ~5%.

Apart from calculating the fractions of binaries and mass transfer phases that could be affected by our treatment of triples, we also attempt to quantify the possible effects of triple breaking on the mass transfer phases. One way in which an outer companion could affect the inner binary is through the Kozai mechanism (Kozai 1962), which can increase the eccentricity of the inner binary and lead to mass transfer. We cannot exclude a priori that by breaking the triples we miss some mass transfer events involving the IMBH. We calculate the timescale for the inner binary to reach maximum eccentricity due to the Kozai mechanism using the initial orbital parameters of the triples (Innanen et al. 1997; Mikkola & Tanikawa 1998; Wen 2003):

$$\tau_{\rm Koz} \simeq 0.16 f \left(\frac{M_i}{M_o^2}\right)^{0.5} \left(\frac{a_o^3}{a_i}\right)^{0.5} \left(1 - e_o^2\right)^{1.5}\ {\rm yr}, \qquad (7)$$

where $f \simeq 0.42 \ln(1/e_{i0})/(\sin^2 i_0 - 0.4)^{0.5}$, e_{i0} and i_0 are the initial inner eccentricity and inclination, respectively, e_o is the outer eccentricity, M_i is the total mass of the inner binary, M_o is the outer companion mass, a_i and a_o are the inner and outer orbital separations, masses are in units of solar masses, and distances are in astronomical units. If $\tau_{\rm Koz}$ is sufficiently short, the outer companion left alone could cause the inner binary to undergo mass transfer at pericenter. However, this would be possible only if $\tau_{\rm Koz}$ is shorter than the collision timescale, $\tau_{\rm coll}$, appropriate for the triple system:

$$\tau_{\rm coll} = \left(1.7 \times 10^3\ {\rm yr}\right) \eta^2 k^{-2} n^{-1} \frac{\langle M\rangle^2}{M_i^2 M_o^2} \times \left(1 + \eta \frac{2}{k} \frac{M_{\rm tot} + \langle M\rangle}{M_i M_o} \langle M\rangle\right)^{-1}, \qquad (8)$$

where $\langle M\rangle$ is the average single star mass, n is the cluster's stellar number density per cubic parsec, and a strong encounter is defined

by the closest approach $d_{\max} \leq ka$, with $k \simeq 2$ (Ivanova et al. 2005). Here η, the hardness of the binary, is defined as

$$\eta = \frac{GM_iM_o}{a_o\sigma^2\langle M\rangle}, \quad (9)$$

where σ is the stellar velocity dispersion. We find that *only* $\sim$11% of all triples have $\tau_{\rm Koz} < \tau_{\rm coll}$. If these systems were not artificially disrupted, they could potentially induce mass transfer through Kozai resonance that is not seen in our simulations. However, we also note that disrupting a triple changes the properties of the inner binary, and this can also lead to mass transfer. We find that about 7% of all tertiary companions are broken before or during a mass transfer phase in inner binaries; this is the maximum fraction of broken triples in our set of standard simulations that could artificially create mass transfer by shrinking the inner binary. Furthermore, we have examined the simulation data and found that there is essentially no overlap between disrupted triples that precede mass transfer and triples with $\tau_{\rm Koz} < \tau_{\rm coll}$. Because the two populations are comparable in size (7% and 11%, respectively), we conclude that these possible effects on mass transfer events more or less mutually cancel.

It should be noted that a small fraction ($\sim$4%–8%) of triple systems form when a tight binary is captured by the IMBH; in this case, the IMBH is recorded as the outer, "ejected" companion and binary evolution is subsequently followed for only the two closely orbiting companions. The data from this small number of unusual disrupted triples are not included in our results and have a negligible effect on the overall IMBH binary evolution.

4. PARAMETER STUDY OF CLUSTERS WITH CENTRAL IMBH

4.1. *IMBH Mass*

Table 4 outlines the evolutionary differences between IMBH masses in model A clusters. The overall increase in companion capture with IMBH mass is apparent. Note that the fractions of both MS and post-MS companions that undergo mass transfer are fairly consistent for all IMBH masses. This underscores the greatly increased likelihood for a post-MS companion to undergo mass transfer compared to a MS companion, independent of external factors. The time fractions spent with a companion of *any* type also increase monotonically with IMBH mass, but because BH companions are more prevalent at higher masses, this behavior is not as clearly seen for MS or post-MS companions. The evolutionary history of a typical single 500 $M_\odot$ simulation is shown in Figure 8 to illustrate the large fraction of its lifetime spent with a companion.

TABLE 4
IMBH Binary Companions: All IMBH Masses

Parameter	Value				
$M_{\rm IMBH}$ ($M_\odot$)	50	100	150	200	500
MC runs[a]	29	167	79	33	44
$\langle N_{\rm comp}\rangle$[b]	2.48	6.49	10.52	12.03	22.66
$\langle N_{\rm MS}\rangle$[c]	2.07	5.90	9.57	11.39	20.98
$\langle N_{\rm post\text{-}MS}\rangle$[c]	0.34	0.47	0.84	0.55	0.98
$\langle N_{\rm MS}^{\rm MT}\rangle$[d]	0.10	0.26	0.46	0.48	0.91
$\langle N_{\rm post\text{-}MS}^{\rm MT}\rangle$[d]	0.14	0.23	0.38	0.21	0.32
MS MT companions[e] (%)	5.00	4.36	4.76	4.25	4.33
Post-MS MT companions[e] (%)	40.00	50.00	45.45	38.89	32.56
$t_{\rm comp}$[f] (%)	24.98	57.63	70.04	76.51	89.69
$t_{\rm MS}$[g] (%)	18.76	40.87	53.69	60.89	56.95
$t_{\rm post\text{-}MS}$[g] (%)	3.59	4.44	4.05	1.77	2.36
$t_{\rm MS}^{\rm MT}$[h] (%)	0.21	2.81	0.76	1.71	2.43
$t_{\rm post\text{-}MS}^{\rm MT}$[h] (%)	0.02	0.11	0.16	0.05	0.10

Note.—All simulations adopt cluster model A.
[a] Number of distinct Monte Carlo simulations evolved to 10^8 yr.
[b] Average number of companions (of any type) per run.
[c] Average number of companions of each type per run. Most post-MS companions are captured while on the MS and do not correspond to different stellar companions.
[d] Average number of MS and post-MS companions that undergo mass transfer per run.
[e] Percent of MS and post-MS companions that undergo mass transfer.
[f] Average percent of total simulation time spent with a companion of any type.
[g] Average percent of time with MS and post-MS companions.
[h] Average percent of time spent in MS and post-MS mass transfer phases.

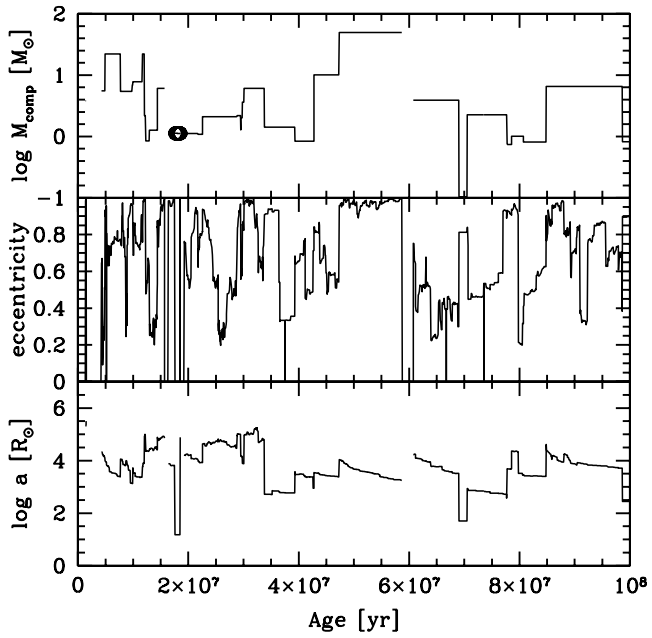

Fig. 8.—Increase in companion acquiring rate for a typical 500 $M_\odot$ simulation over a 100 $M_\odot$ simulation (cf. Fig. 1); the IMBH has a companion for almost all of its lifetime. *Top*, companion mass; *middle*, eccentricity; *bottom*, orbital separation.

A clear result in Table 4 is that 50 $M_\odot$ IMBHs have a very low rate of companion capture and mass transfer events. This places a lower limit on the IMBH mass likely to form a luminous X-ray binary. For higher IMBH masses, we emphasize as in § 3.4 that the average mass transfer time fractions are typically dominated by a few simulations with very long mass transfer phases. Consequently, we do not observe any significant difference in $t_{\rm MS}^{\rm MT}$ or $t_{\rm post\text{-}MS}^{\rm MT}$ over the range of IMBH masses.

As in 100 $M_\odot$ IMBH clusters, X-ray luminosities for other IMBH masses produce transient or persistent ULXs for insignificant fractions of the cluster lifetime, except possibly for 500 $M_\odot$. Clusters with 500 $M_\odot$ IMBHs do spend significantly more of their mass transfer time as ULX sources; these systems are transient for $\simeq$40% of the mass transfer time and persistent ULXs for $\simeq$12% of the mass transfer time. Even so, these ULXs would be observable for only $\simeq$0.35% of the total cluster lifetime.

The rate of triple system formation increases monotonically with IMBH mass (Fig. 7 and Table 5). Clusters with a 50 $M_\odot$ IMBH have very few triple systems, as is expected based on their low rate of IMBH binary formation. 500 $M_\odot$ IMBHs have by far the highest average rate of triple formation. In fact, more tertiary systems than binary systems form in this case, in a ratio of 1.6 : 1 compared to 0.5 : 1 for 100 $M_\odot$ simulations (Table 5). Our artificial treatment of triples limits our ability to reliably analyze clusters with an IMBH $\gtrsim$500 $M_\odot$. In the 100–200 $M_\odot$ range, we

TABLE 5

Triple Systems and IMBH Companions: All IMBH Masses

Parameter	Value				
$M_{\rm IMBH}$ ($M_\odot$)	50	100	150	200	500
MC runs[a]	20	109	53	16	39
$\langle N_{\rm trip}\rangle$[b]	0.90	3.46	7.98	9.44	35.59
$\langle N_{\rm trip}/N_{\rm bin}\rangle$[c]	0.38	0.50	0.75	0.81	1.58
Close triples[d] (%)	50.00	28.90	18.91	26.49	22.05
Affected MT companions[e] (%)	66.67	47.72	62.22	33.33	71.43
Close MT companions[f] (%)	0.00	10.24	13.33	6.67	20.41
$t_{\rm MT}$[g] (%)	0.32	1.60	1.11	1.00	2.02
$t_{\rm aff}^{\rm MT}$[h] (%)	3.13	21.07	41.82	25.16	67.08
$t_{\rm close}^{\rm MT}$[i] (%)	0.00	4.96	7.57	0.00	27.14

Note.—All simulations adopt cluster model A.

[a] Number of distinct Monte Carlo simulations for which triples data were obtained (note that Tables 3 and 5 are based on smaller sample sizes than are other data).

[b] Average number of unique triple systems per run.

[c] Average ratio of distinct triple systems to distinct binary systems formed.

[d] Percent of triples that are "close" ($p_{\rm out}/a_{\rm in} \leq 3$).

[e] Percent of mass transfer companions that are potentially affected by one or more tertiary companions gained during their lifetime.

[f] Percent of mass transfer companions that are potentially affected by one or more close tertiary companions gained during their lifetime.

[g] Percent of total simulation time spent in mass transfer phases.

[h] Percent of total mass transfer time potentially affected by triples.

[i] Percent of total mass transfer time potentially affected by close triples.

do not find any conclusive pattern in the percentage of triples with close orbits or in the percentage of mass transfer affected by triples.

4.2. *Cluster Models*

To determine the dependence of our results on initial cluster conditions, we test two variations of our standard cluster model, as outlined in Table 1. We use our standard IMBH mass of 100 $M_\odot$ for all these simulations.

In model C, when a lower number density is used ($n_c = 10^4$ pc^{-3}), the IMBH has a companion for only ~35% of its evolution time, about half the companion time fraction calculated for the higher density model (Table 6). The IMBH spends only a fraction of a percent of total simulation time with mass-transferring companions (0.53%). We conclude that clusters with our standard core number density, $n_c = 10^5$ pc^{-3}, are much more likely to contain an accreting IMBH ULX.

IMBH companions in clusters with a flattened IMF (model B) are slightly more massive, as expected, with most between ~1 and 10 $M_\odot$ (Fig. 9). The IMBH has a binary companion for a shorter time fraction (40%) than in model A simulations (Table 6). A decrease is also seen in the mass transfer time fraction between the two models. This could possibly result from having more massive stars in the core, due to the flatter IMF, that interact with and can disrupt IMBH binaries. However, we caution again that the mass transfer time fraction for our standard model is dominated by a few outliers, so the difference seen in model B may or may not be significant.

The time in which the model B clusters are observable as ULX sources is very short, as in model A clusters: a transient ULX forms for about 3.5% of the total mass transfer time, and persistent mass transfer at ULX luminosities occurs for about 7% of the mass transfer time. These imply a possible ULX time fraction of <0.05%. Furthermore, the behavior of triple systems in model B is qualitatively and quantitatively similar to that of triple systems in standard model clusters.

Small differences can be seen when 3BBF is allowed in the cluster. 3BBF enhances the rate at which massive objects can grow through collisions, since the hard formed binaries can collide with other formed binaries. As a result, companions are a bit more massive in clusters with 3BBF (Fig. 9). The difference in the mass distributions is small, but a larger effect is seen in the mass transfer time fraction. The time the IMBH spends with a mass-transferring companion decreases by more than half when 3BBF is included. This phenomenon is probably similar to that

TABLE 6

IMBH Binary Companions: All Cluster Models

Parameter	Value				
Model	A	A+	B	B+	C
MC runs[a]	167	12	102	19	37
$\langle N_{\rm comp}\rangle$[b]	6.49	7.75	4.35	4.32	2.16
$\langle N_{\rm MS}\rangle$[c]	5.90	6.92	3.15	3.05	2.03
$\langle N_{\rm post\text{-}MS}\rangle$[c]	0.47	0.50	0.59	0.58	0.13
$\langle N_{\rm MS}^{\rm MT}\rangle$[d]	0.26	0.50	0.16	0.21	0.05
$\langle N_{\rm post\text{-}MS}^{\rm MT}\rangle$[d]	0.23	0.25	0.21	0.21	0.03
MS MT companions[e] (%)	4.36	7.23	4.97	6.90	2.67
Post-MS MT companions[e] (%)	50.00	50.00	35.00	36.36	20.00
$t_{\rm comp}$[f] (%)	57.63	61.43	40.35	39.82	34.71
$t_{\rm MS}$[g] (%)	40.87	48.90	18.88	23.19	32.35
$t_{\rm post\text{-}MS}$[g] (%)	4.44	5.56	4.69	2.10	0.50
$t_{\rm MS}^{\rm MT}$[h] (%)	2.81	1.43	0.54	0.17	0.52
$t_{\rm post\text{-}MS}^{\rm MT}$[h] (%)	0.11	0.05	0.04	0.07	0.01

Notes.—See Table 1 for the details of each model. Models A+ and B+ are identical to A and B, but with 3BBF allowed.

[a] Number of distinct Monte Carlo simulations evolved to 10^8 yr.

[b] Average number of companions (of any type) per run.

[c] Average number of companions of each type per run. Most post-MS companions are captured while on the MS and do not correspond to different stellar companions.

[d] Average number of MS and post-MS companions that undergo mass transfer per run.

[e] Percent of MS and post-MS companions that undergo mass transfer.

[f] Average percent of total simulation time spent with a companion of any type.

[g] Average percent of time with MS and post-MS companions.

[h] Average percent of time spent in MS and post-MS mass transfer phases.

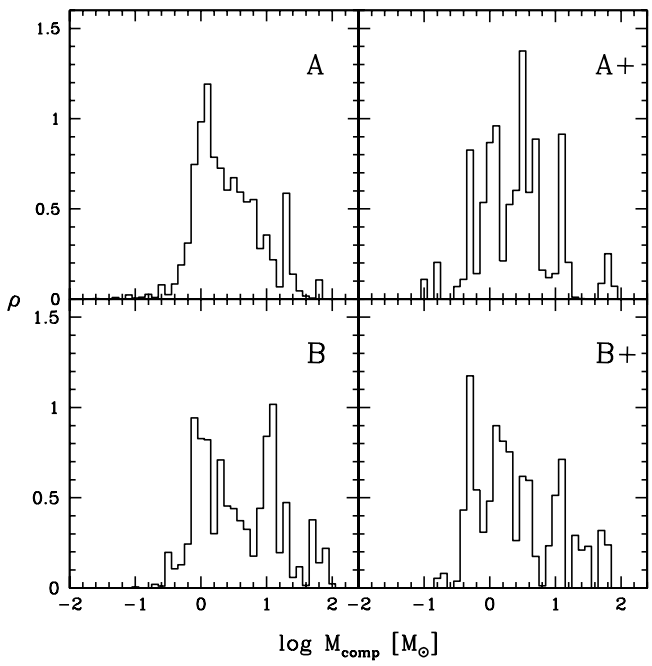

Fig. 9.—Probability density of companion mass at each time step, shown for cluster models A (167 runs), B (102 runs), A+ (12 runs), and B+ (19 runs).

causing the disparity in mass transfer time between model A and B clusters.

Due to the 100% initial binary fraction, we do not need 3BBF to form binaries. Overall, we see that our cluster models are qualitatively similar with and without 3BBF, so we conclude that we can safely omit 3BBF from our simulations.

5. DISCUSSION

We have undertaken the first detailed investigation of IMBH interactions in young ($\simeq$100 Myr), dense cluster cores, incorporating binary dynamics with full binary star evolution. Specifically, we study the prevalence and characteristics of interacting binaries involving the central IMBH, and we examine and can better understand their role as potential ULX sources. We use numerical cluster simulations that simplify some aspects of detailed dynamical evolution and allow us to focus on individual core stellar interactions while largely ignoring long-term cluster evolution. We analyze our results in terms of the frequency of IMBH binaries formed and their properties, the frequency of associated mass-transferring IMBH binaries, and the associated X-ray luminosities expected. With our cluster model A, we explore an IMBH mass range of 50–500 $M_{\odot}$, and we study two variations on this model as well (Table 1). Finally, we analyze the nature of triple systems formed as a possible influence on our results here and as a guide for designing future simulations.

Our main results are summarized as follows:

1. IMBHs more massive than 100 $M_{\odot}$ in model A clusters spend the majority (>50%) of their evolution time with a binary companion.
2. Mass-transferring IMBH companions are relatively rare ($\simeq$3% of the IMBH evolution time on average) compared to the total time the IMBH spends with a companion, but when they do occur, the mass transfer persists for relatively long times.
3. IMBHs spend more time in mass transfer phases with MS companions than with post-MS companions.
4. A much larger number fraction of post-MS companions than MS companions undergo mass transfer.
5. In model A clusters, IMBH binaries are found to be persistent X-ray sources for about 90% of the total mass transfer time, but the X-ray luminosity reaches ULX values ($L_X > 10^{39}$ ergs s^{-1}) for only $\sim$2% of the mass transfer time. For the rest of the mass transfer time ($\simeq$10%), IMBH binaries are found to be transients, which have short duty cycles. Given that the typical total mass transfer time is $\simeq$3% of the IMBH evolution time, these results amount to a vanishingly small observable-ULX time fraction (<1%) over the lifetime of the young clusters we consider.
6. Higher mass IMBHs capture more companions throughout their evolution, making them more likely in a statistical sense to capture a companion that can overflow its Roche lobe.
7. Model A clusters with a 50 $M_{\odot}$ IMBH and cluster model C have very few mass-transferring IMBH binaries.
8. In model B clusters, the IMBH spends less time with a companion (40% of the total time) and less time in mass transfer (<1% of the total time) than in Model A clusters.
9. For all cluster models and IMBH masses explored here, the possible ULX time fraction of the cluster lifetime (100 Myr) is found to be typically $\sim$0.1% or even smaller.

We note that results presented by Hopman et al. (2004) imply a higher incidence of possible ULX activity associated with MS companions to central IMBHs (typically with a duration of $\gtrsim 10^7$ yr). However, these calculations are based on analytical estimates of the possible tidal capture rates (assuming the most optimistic conditions for tidal capture) for an IMBH in a cluster of single MS stars and the subsequent *isolated* binary evolution of MS companions. We do allow for tidal captures in our simulations (for details of implementation see Ivanova et al. 2005), but they turn out to be a negligible contributor to the rate at which IMBHs acquire companions (exchanges into binaries is by far the dominant process). This difference is most likely due to the lower IMBH mass range we explore. The binary evolution calculations of Hopman et al. (2004) are not integrated with any dynamical evolution (analytically or numerically), and, based on our results, we conclude that the assumption of isolated evolution is not realistic. Given the substantial differences in calculation methods, however, it is not possible to make direct and quantitative comparisons between this study and our study. We further note that our conclusions about the low probability of ULX formation are in agreement with a recent study by Madhusudhan et al. (2006), who investigated binary mass transfer sequences with an IMBH.

Last, we recognize triple systems as one possibly limiting factor in our simulations. Since triples are artificially disrupted as they form, we examine the influence of triples in terms of their initial orbital parameters and their coincidence with mass transfer phases. We find that while a large number of triple systems form per simulation, and while about $\frac{1}{3}$–$\frac{2}{3}$ of all 100–200 $M_{\odot}$ mass-transferring companions do coincide with triple system formation, only a small fraction of mass transfer phases are affected by triples with "close" orbits. Furthermore, two opposing phenomena related to triple breaking may cause some uncertainties. Mass transfer may be prevented when potential Kozai evolution is artificially interrupted, or it may be artificially induced when release of the outer companion shrinks the inner binary. We find that both effects are relevant for only small, roughly equivalent fractions of triples, causing a negligible net impact on our mass transfer results. Therefore, we conclude that our treatment of triples in the regime of IMBH masses considered here does not influence our conclusions about the possibility of IMBH ULX formation. However, given the higher occurrence of triples in our 500 $M_{\odot}$ runs, the issues of multiples and cusp formation are most probably more important for more massive IMBHs ($\gtrsim$500 $M_{\odot}$) than those considered here.

For these more massive IMBHs, a more physical treatment of multiple systems would in principle allow the remaining uncertainties regarding triples, multiples, and the ultimate formation of central cusps to be resolved. However, to examine ULX formation, treatment of the stellar evolution of multiple systems cannot be ignored (especially when it involves massive-star companions that lose mass in winds, experience core collapse, and can themselves disrupt orbits and alter dynamical evolution). Simulations that incorporate all of these effects are simply not possible at present. Instead, for our future explorations of the IMBH-ULX connection in dense clusters, we plan to implement simulations that would represent an improvement over those presented here. Such future calculations could differentiate between triple systems in which the inner binary may be disturbed and those in which the outer companion can be ignored. In the latter case, the third companion would be kept in the system and its dynamical evolution alone could be simulated, while full stellar evolution and dynamics are calculated for the inner binary.

We thank Marc Freitag for valuable discussions on cluster dynamics and cluster properties before and after IMBH formation. This work is supported by a David and Lucile Packard Foundation Fellowship in Science and Engineering grant, NASA ATP grant NAG5-13236 and LTSA grant NAG5-13056 to V. Kalogera, NASA *Chandra* Theory Award NAS8-03060 to N. Ivanova, and NASA ATP grant NAG5-12044 to F. Rasio.

REFERENCES

Apai, D. 2004, Ph.D. thesis, Univ. Heidelberg
Bacon, D., Sigurdsson, S., & Davies, M. B. 1996, MNRAS, 281, 830
Bahcall, J. N., & Wolf, R. A. 1976, ApJ, 209, 214
Baumgardt, H., Makino, J., & Ebisuzaki, T. 2004, ApJ, 613, 1143
Belczynski, K., Kalogera, V., & Bulik, T. 2002, ApJ, 572, 407
Belczynski, K., Kalogera, V., Rasio, F. A., Taam, R. E., Zezas, A., Bulik, T., Maccarone, T. J., & Ivanova, N. 2006, ApJS, submitted (astro-ph/0511811)
Belczynski, K., Sadowski, A., & Rasio, F. A. 2004, ApJ, 611, 1068
Colbert, E., & Miller, M. C. 2006, in Tenth Marcel Grossmann Meeting on General Relativity, ed. M. Novello, S. Perez-Bergliaffa, & R. Ruffini (Singapore: World Scientific), in press (astro-ph/0402677)
Colbert, E., & Mushotzky, R. 1999, ApJ, 519, 89
Colbert, E., & Ptak, A. 2002, ApJS, 143, 25
Delgado-Donate, E. J., Clarke, C. J., Bate, M. R., & Hodgkin, S. T. 2004, MNRAS, 351, 617
Di Stefano, R., & Rappaport, S. 1994, ApJ, 437, 733
Dubus, G., Lasota, J., Hameury, J., & Charles, P. 1999, MNRAS, 303, 139
Fabbiano, G. 1989, ARA&A, 27, 87
Fabbiano, G., & White, N. 2006, in Compact Stellar X-Ray Sources, ed. W. H. G. Lewin & M. van der Klis (Cambridge: Cambridge Univ. Press), in press (astro-ph/0307077)
Fabbiano, G., Zezas, A., & Murray, S. S. 2001, ApJ, 554, 1035
Fregeau, J. M., Cheung, P., Portegies Zwart, S. F., & Rasio, F. A. 2004, MNRAS, 352, 1
Freitag, M., Gürkan, M. A., & Rasio, F. 2006a, MNRAS, submitted (astro-ph/0503130)
Freitag, M., Rasio, F. A., & Baumgardt, H. 2006b, MNRAS, submitted (astro-ph/0503129)
Gürkan, M. A., Freitag, M., & Rasio, F. 2004, ApJ, 604, 632
Hills, J. G. 1984, AJ, 89, 1811
Hopman, C., Portegies Zwart, S. F., & Alexander, T. 2004, ApJ, 604, L101
Hut, P., McMillan, S., & Romani, R. W. 1992, ApJ, 389, 527
Innanen, K. A., Zheng, J. Q., Mikkola, S., & Valtonen, M. J. 1997, AJ, 113, 1915
Ivanova, N., Belczynski, K., Fregeau, J. M., & Rasio, F. A. 2005, MNRAS, 358, 572
Ivanova, N., & Kalogera, V. 2006, ApJ, 636, 985
Kaaret, P., Prestwich, A. H., Zezas, A., Murray, S. S., Kim, D. W., Kilgard, R. E., Schlegal, E. M., & Ward, M. J. 2001, MNRAS, 321, L29
Kalogera, V., Henninger, M., Ivanova, N., & King, A. R. 2004, ApJ, 603, L41
King, A. R., Davies, M. B., Ward, M. J., Fabbiano, G., & Elvis, M. 2001, ApJ, 552, L109
King, A. R., Kolb, U., & Burderi, L. 1996, ApJ, 464, L127
Kozai, Y. 1962, AJ, 67, 591
Kroupa, P. 2002, Science, 295, 82
Levine, J. L., Lada, E. A., & Elston, R. J. 1999, BAAS, 31, 1490
Lira, P., Lawrence, A., & Johnson, R. 2000, MNRAS, 319, 17
Madhusudhan, N., Justham, S., Nelson, L., Paxton, B., Pfahl, E., Podsiadlowski, P., & Rappaport, S. 2006, ApJ, 640, 918
Mardling, R. A., & Aarseth, S. J. 2001, MNRAS, 321, 398
Matsumoto, H., Tsuru, T. G., Koyama, K., Awaki, H., Canizares, C. R., Kawai, N., Matsushita, S., & Kawabe, R. 2001, ApJ, 547, L25
McClintock, J. E., & Remillard, R. A. 2006, in Compact Stellar X-Ray Sources, ed. W. H. G. Lewin & M. van der Klis (Cambridge: Cambridge Univ. Press), in press
Merritt, D., & Szell, A. 2006, ApJ, submitted (astro-ph/0510498)
Mikkola, S. 1983, MNRAS, 203, 1107
Mikkola, S., & Tanikawa, K. 1998, AJ, 116, 444
Miller, J. M., Fabbiano, G., Miller, M. C., & Fabian, A. C. 2003, ApJ, 585, L37
Miller, J. M., Fabian, A. C., & Miller, M. C. 2004a, ApJ, 607, 931
Miller, J. M., Zezas, A., Fabbiano, G., & Schweizer, F. 2004b, ApJ, 609, 728
Mitsuda, K., et al. 1984, PASJ, 36, 741
Mucciarelli, P., Zampieri, L., Falomo, R., Turolla, R., & Treves, A. 2005, ApJ, 633, L101
Mushotzky, R. 2004, Prog. Theor. Phys. Suppl., 155, 27
Pakull, M. W., & Mirioni, L. 2001, Astronomische Gesellschaft Meet. Abs., 18, 112
Patruno, A., Colpi, M., Faulkner, A., & Possenti, A. 2005, MNRAS, 364, 344
Portegies Zwart, S. F., Hut, P., McMillan, S., & Verbunt, F. 1997a, A&A, 328, 143
Portegies Zwart, S. F., Hut, P., & Verbunt, F. 1997b, A&A, 328, 130
Portegies Zwart, S. F., Makino, J., McMillan, S., & Hut, P. 1999, A&A, 348, 117
Portegies Zwart, S. F., & McMillan, S. 2002, ApJ, 576, 899
Ptak, A., & Colbert, E. 2004, ApJ, 606, 291
Rappaport, S. A., Podsiadlowski, P., & Pfahl, E. 2005, MNRAS, 356, 401
Rasio, F. A., Pfahl, E. D., & Rappaport, S. 2000, ApJ, 532, L47
Roberts, T., & Warwick, R. 2000, MNRAS, 315, 98
Sigurdsson, S., & Phinney, E. S. 1995, ApJS, 99, 609
Spitzer, L. 1987, Dynamical Evolution of Globular Clusters (Princeton: Princeton Univ. Press)
Strohmayer, T., & Mushotzky, R. 2003, ApJ, 586, L61
Trenti, M., Ardi, E., Mineshige, S., & Hut, P. 2006, ApJ, submitted (astro-ph/0508517)
Wen, L. 2003, ApJ, 598, 419